Journal of Interventional Medicine 3 (2020) 1–16

HOSTED BY

ELSEVIER

Contents lists available at ScienceDirect

Journal of Interventional Medicine

journal homepage: www.keaipublishing.com/cn/journals/journal-of-interventional-medicine/

Application of three-dimensional printing in interventional medicine

Geng Zhou [a], Weidong Liu [b], Yi Zhang [a], Wenquan Gu [b], Minghua Li [c], Chuan Lu [d], Ran Zhou [e], Yichen Che [f], Haitao Lu [c], Yueqi Zhu [c], Gaojun Teng [a], Yongde Cheng [g,*]

[a] Center of Interventional Radiology & Vascular Surgery Department of Radiology, Zhongda Hospital, Medical School, Southeast University, Nanjing, 210000, China
[b] Shanghai Punan Hospital International Medical Department, Shanghai, 200125, China
[c] Department of Radiology, Shanghai Jiao Tong University Affiliated Sixth People's Hospital, Shanghai, 200233, China
[d] School of Radiology, Taishan Medical College, Shandong, 271016, China
[e] Department of Ultrasonography, Zaozhuang Mining Group Central Hospital, Zaozhuang, Shandong, 277800, China
[f] Department of Ultrasonography, Maternity & Child Health Hospital of Mudan District, Heze, Shandong, 274000, China
[g] Department of Radiology, No.85 Hospital of PLA, Shanghai, 200052, China

Introduction

In recent years, three-dimensional printing (3DP), an additive manufacturing process, has gained widespread clinical application, and 3DP has been considered as the third industrial revolution.[1] In its early introduction in the 1980s, 3DP served as a software-controlled technology that converted computer-aided-design (CAD) data into a physical object via a single process. By depositing multiple two-dimensional cross-sections one above the other, 3DP can now be used to build arbitrarily complex geometries and patient-specific constructs using the patient's imaging data. Till date, computed tomography has been the main imaging data source for 3DP owing to its excellent spatial resolution. Furthermore, current 3D printers have enabled bedside on-demand fabrication of medical products in hospitals. New materials including polymers, ceramics, biomaterials, and metals have been developed for such applications over the last few decades. Medical fields that employ 3DP technologies have also expanded, such as tissue engineering, regenerative medicine, pharmaceutics, and medical models and devices.[2] The market for additive manufacturing is expected to surpass $20 billion in the global industry by the end of the 2020.[3] Although the use of 3DP technology in interventional medicine is still relatively new, advancements are occurring within this discipline at a rapid rate. Different 3DP technologies, materials, and clinical applications relevant to the interventional field are discussed in this article.

Technologies in 3D printing

ISO (international standardization organization) standards currently recognize several methods for additive manufacturing, all of which have been adapted for medical use. These processes include vat photopolymerization, material extrusion, material jetting, powder bed fusion, binder jetting, and direct energy deposition (Table 1).[3,4]

Laser based 3D printing

Stereolithography

Stereolithography (SLA) systems are the most widely used type of 3DP. Chuck Hull invented the first SLA printing machine in 1986 and commercialized it 2 years later.[3] In SLA printing, an ultraviolet (UV) laser (of wavelength 300–400 nm) is used to scan and cure thin layers of liquid material, e.g., photocurable resin, one above the other at the surface of a vat. The material is then hardened using a scanning laser or digital light processing projection (also known as continuous-liquid-interface production), and the base is shifted down in the z-direction by one layer. This process is repeated until the structure is completely fabricated. SLA offers a spatial resolution of up to 25 μm with a minimum structure size of 300 μm.[6] A disadvantage of SLA is that the printing materials are required to be photocrosslinkable. Several biocompatible biomaterials, such as poly (propylene fumarate), poly (D, L-lactide), and poly (e-caprolactone) (PCL), have been used in SLA.[7]

Two-photon polymerization

Two-photon polymerization (TPP) comprises the use of a near-infrared femtosecond laser to initiate the fabrication directly inside the photosensitive resin. In SLA, the polymerization process takes place at the surface of a photosensitive resin. It is only possible to build 3D structures layer by layer. However, in TPP, two photons are absorbed simultaneously by a photoinitiator and act as a single photon to start the polymerization. This allows the laser to directly build polymeric 3D objects into the volume of the photosensitive material. Furthermore, TPP provides a much higher resolution (less than 100 nm) than most 3DP methods. However, the application of TPP is also limited to photopolymerizable materials. TPP has many medical applications in tissue engineering, microdevices, and drug delivery (Fig. 1).[6,8]

* Corresponding author.
E-mail address: yongdech@163.com (Y. Cheng).

https://doi.org/10.1016/j.jimed.2020.01.001

Available online 21 January 2020

Please cite this article as: Zhou G et al., Application of three-dimensional printing in interventional medicine, Journal of Interventional Medicine, https://doi.org/10.1016/j.jimed.2020.01.001

Table 1
Overview of 3DP technologies, materials, and fabrication parameters.

Technology	Material category	Available material	Layer thickness (μ m)	Temperature stability (°C)
SLA	Liquid-photopolymers Ceramics	Elastomers, epoxy resins, ceramic particles in liquid resins (silica, alumina, zirconia)	50–250	80
SLS	Plastic powder Ceramic powder Composites	Polyamid, polystyrene thermoplastic polyurethane Bioglass, silica, zirconia, alumina, sands, graphite Composite materials (Alumide, ceramic–ceramic, polymer-matrix)	100–200	80–150
SLM	Metal powder	Stainless steel, tool steel, aluminum, titanium, cobalt-chrome	20–200	350–1000
EBM	Metal powder	Titanium, cobalt-chrome	50–100	500–1000
FDM	Plastic filament Composites	ABS Polylactids, waxes	100–1000	80
2PP	Photoresists	SU-8, OrmoComp	<1	100–300
PolyJet (PJ)	Acryl-photopolymers	VeroClear, VeroWhite, TangoBlack, ABS	16–32	50
Multijet modeling (MJM)	Acryl-photopolymers	VisiJet family (polycarbonat-like)	16–32	50
3D-Printing (3DP)/ Binder Jetting (BJ)	Chalky powder Ceramics Composites	Zirconia, silica, sands, Ti3SiC2 Zirconia, silica, sands, Ti3SiC2, Ti3SiC2 Ceramic-ceramic, polymer-ceramic	150–500	115

Modified from Krujatz F. et al., N Biotechnol[5].
SLA = stereolithography; SLS = selective laser sintering; SLM = selective laser melting; EBM = extrusion-based methods; FDM = fused deposition modelling; 2PP = two-photon polymerization.

Powder-fusion printing

In powder-fusion printing (PFP), granular materials such as plastic, polymer, ceramic, or metal particles in a powder bed are locally heated and fused with a laser beam or electron beam into thin layers. PFP technologies include selective laser sintering (SLS), selective laser melting (SLM), and electron beam melting.[2] After a layer has been printed, a new layer of powder is spread across the bed and selectively sintered. To facilitate the spreading of the powder, the granules used in this printing method typically have diameters between 10 μm and 100 μm. The powder left unfused serves as a support material during the building process and is removed and recycled after the fabrication is complete. The sintering process (e.g., SLS) provides a porous structure and a rough surface, in contrast to the melting process (e.g., SLM), which provides a higher density and mechanical strength.[9] SLS was invented in 1986 by Carl Deckard and is now used for the production of tissue-engineered scaffolds in clinical applications.[10] As in the case of SLA, the resolution of the SLS techniques is dependent on the diameters of the laser and the powder particles. One of the significant advantages of SLS is the vast range of materials that it can be used with. SLS has recently gained popularity in patient-specific medical-device production and in-hospital printing.[11]

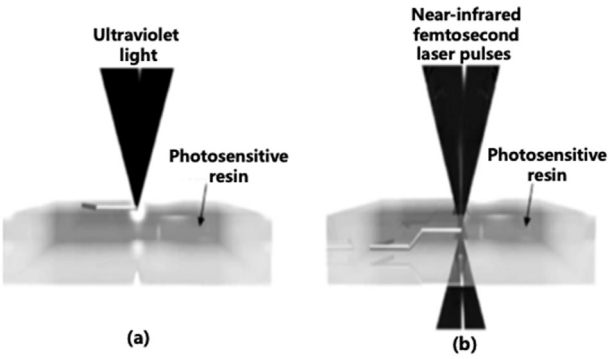

Fig. 1. Schematic showing SLA printing at the surface of a photosensitive polymer (a) and TPP printing at the focal point inside the resin volume (b).[6]

Extrusion-based methods

Extrusion-based methods (EBM) comprise the use of an extrusion nozzle to selectively deposit material in a layer-wise fashion to fabricate the desired 3D object. Different materials are supplied as a filament through the extrusion head. EBM bioprinting is the most common technique used in the medical field. The EBM 3DP technologies used in medicine include fused deposition modeling (FDM) and direct ink writing (DIW).

Fused deposition modeling

Fused deposition modeling (FDM) was first introduced in 1989 by Scott Crump.[3] FDM comprises the use of a pressure-driven system to push molten material through a heated printing head onto a stage layer by layer. As the material is deposited, it cools and solidifies to form the 3D object. FDM is currently the cheapest 3DP method and can be used to process almost all types of thermoplastic polymers. Acrylonitrile butadiene styrene (ABS), polylactic acid (PLA), and biomedical materials, such as hydrogels and some polymer–ceramic hybrids (polycaprolactone with bioactive glass), are commonly used in FDM. FDM is based on surface chemistry, thermal energy, and layer manufacturing technology. FDM can be used to fabricate implants, prostheses, anatomical models,

Fig. 2. Picture showing the fused deposition modeling 3D printer (MakerBot Replicator 2 Desktop 3D Printer).[13]

and surgical guides for personalized medicine. Cells or bioactive molecules are not suitable for the FDM process (Fig. 2).[12,13]

Direct ink writing

Direct ink writing (DIW) was reported by Lewis et al. and has been proven to be advantageous for printing biomaterial structures for applications in tissue engineering and biomedical implants.[14] DIW is similar to the FDM approach and is an extrusion-based technique in which soft material is delivered through a disposable nozzle. Viscoelastic inks are extruded in the form of a continuous filament, which is consolidated via chemical reactions or a physical mechanism shortly after its deposition in the printing tray. The nozzle's diameter limits the resolution of the printed fibers. The ink must be sufficiently fluid to allow for smooth extrusion and have sufficient strength to facilitate the building of an undistorted structure. The conventional inks for DIW 3DP are elastomers and hydrogels. DIW is particularly suitable for the printing of cell-laden (bioink) structures. Structural instabilities are a limitation of the DIW 3DP approaches (Fig. 3).[15,16]

Inkjet-based 3D printing

Inkjet-based 3D printing (IBP) method is a non-contact technique in which jet-ink materials comprising low-viscosity droplets are allowed to solidify on a tray. The printing materials are deposited via thousands of small print heads that are similar to those used in commercial inkjet printers; however, photoresin or glue (such as binder-jetting) is jetted out in IBP instead of ink. Once the material is solidified, the printing tray is lowered, and the next layer is printed. Compared to the continuous filaments produced in EBM techniques, the IBP system can generate a higher resolution and more delicate structures. The IBP method also offers compositional control and facilitates the fabrication of heterogeneous items comprising individual voxels of different properties. Moreover, instead of a photoreactive polymer, binder or glue can be jetted onto powder beds to locally bind particles together in a method similar to SLS printing.[3,17,5]

Currently, the cost of a 3DP printer ranges in thousands of USD, and some equipment can be purchased at a few hundred USD. However, 3D printers that have a very high resolution and multi-material printing capabilities can be prohibitively expensive. The majority of fabrications cost approximately USD 100–200 based on the complexity of the required structure and the materials used.[18] In emergent situations, such as intracerebral hemorrhages, a model can be printed in less than 60 min.[19]

Modalities of bioprinting

3D bioprinting is a fabrication technology used to precisely place cell-laden biomaterials for the construction of functional tissues or artificial organs (Table 2).[20]

Table 2
Summary of 3D bioprinting technologies.

3D bioprinting technologies			
	DBB	EBB	LBB
Resolution	Medium (~100 μm)	Low (~200 μm)	High (~20 μm)
Droplet size	50–300 μm	100 μm–1 mm	20 μm
Printing speed	Fast (1–10000 droplets/s)	Medium (10–1000 μm/s)	Medium (200–1600 μm/s)
Preparation time	Short	Medium	Long
Cell viability	Medium-high (80–90%)	Medium (40–90%)	High (>95%)
Cell density	Low ($<10^6$/ml)	High	Medium ($\sim10^8$/ml)
Structure stability	Poor	Good	Fair
Bioink	Cell suspension	Viscous material	Both
Bioink viscosity mPa s^{-1}	3.5–12	30–6x10^7	1–300
Cost	Low	Medium	High
Throughput of printing	High	Medium	Low
Advantages	Low cost; high resolution; high throughput; gradients can be generated by altering droplet size	High cell density at physiological level; sample process; ability of printing large structure; good reproducibility	High resolution; single-cell manipulation; low shear stress on cell; no clogging associated with nozzles; wide viscosity range
Disadvantages	Easy nozzle clogging; low droplet directionality; can print using only low-viscosity ink; high shear force can cause cell deformation	Low resolution; low cell viability due to high shear force; nozzle clogging; low speed; limited biomaterial	High cost; time-consuming; technically challenging; limited printing volume; low throughput; low cell density

DBB indicates droplet-based bioprinting; EBB = extrusion-based bioprinting; LBB = Laser-based bioprinting. (Modified from: Borovjagin AV, et al. Circ Res. 2017.[20])

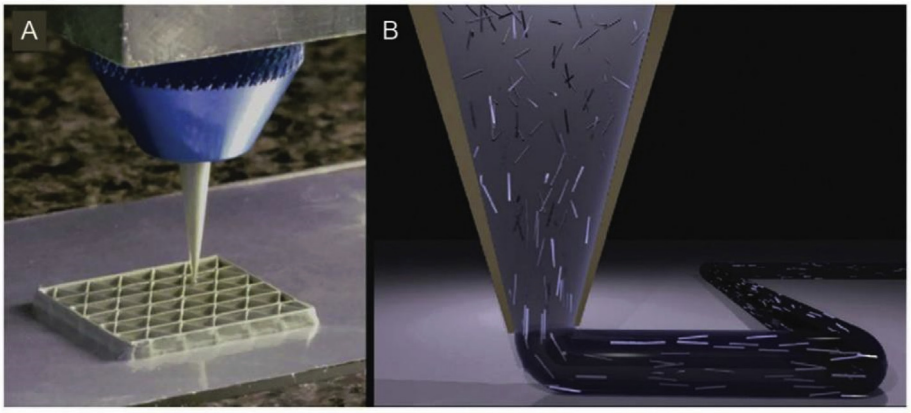

Fig. 3. Schematic of the nozzle in DIW printer.[16]

Droplet-based bioprinting

Droplet-based bioprinting (DBB) is a cellular bioprinting technique based on traditional 2D technology and was introduced in 2003.[21] Inkjet-based 3D printers (also known as drop-on-demand printers) are one of the most commonly used bioprinters. Bioinks consist of biomaterials such as living cells, biologics, and bio-chemicals. Inkjet-based bioprinters use thermal or acoustic forces to eject the droplets onto the supporting substrate. The deposited droplets can be polymerized via crosslinking mechanisms, such as the use of crosslinking agents, pH, and UV radiation, to form 3D objects. The minimum cell viability in DBB is generally greater than 70%.[22]

Extrusion-based bioprinting

Extrusion-based bioprinting (EBB) technology is based on the continuous extrusion and rapid polymerization of hydrogel filaments of bioinks. Mechanically driven extrusion systems of EBB deposit cell-support materials in the form of hydrogel solutions. EBB can be used for depositing materials with a high cell concentration to accelerate tissue growth and formation. One key area of research is in situ bioprinting, which comprises printing cells and biomaterials directly into the wounds of a patient.[23] However, the high dispensing pressure and shear stresses in this process can be detrimental for the deposited cells and decrease their viability. Multiple cell types can be bioprinted in a spatially organized manner, thus mimicking in vivo organization.[24]

Laser-based bioprinting

Laser-based bioprinting (LBB) technologies comprise the use of laser energy (focused laser beam) for transferring and arranging biomaterials. There are many different forms of LBB 3D bioprinting. In LBB printing, single cells or cell suspensions are placed onto the biological material side of a donor slide. A laser pulse is used to locally heat the energy-absorbing side of the donor slide to create a bubble. Subsequently, the microbubble bursts and generates shock waves that propel the cell containing materials from the donor slide onto a collector substrate, where the fabrication takes place. The laser scan is repeated to fabricate a multilayered construct with precise cellular deposition at specific positions. This process is time-consuming for large tissue printing. Furthermore, using this technique, the cells may suffer from metal contamination (Fig. 4).[25,26]

3D bioprinting offers very precise control on the placement of cells, proteins, DNA, drugs, growth factors, and other bioactive substances to better reproduce the structural and functional complexity of living tissue/organs comprising vasculature and neural networks.[27] The demand for clinically transplantable organs is likely to be met by the application of 3D bioprinting techniques in the tissue engineering field. However, the complexity of the physiological and biological behavior of tissues creates challenges for successful tissue regeneration. Current research in the 3D-printed organ field is focused on the fabrication of vascularized tissue for the diffusion of oxygen and nutrients.

4D printing

The development of 3DP and smart materials has led to the new concept of four-dimensional (4D) printing. 4D printing is based on the use of photo- or thermal-responsive shape memory polymers (SMPs) and FDM printing technology. 4D printing is 3DP with the additional dimension of time. SMPs are a class of unique polymeric materials that can be used to memorize a permanent shape. Environmental stimuli, such as temperature, electricity, pH, or light, could trigger the shape recovery behavior of 4D printed devices, which would then recover from their temporary form to their original shape.[28] The 4D printing strategy could provide opportunities for the production of smart medical devices and even biologically active constructs. Currently, the majority of the 4D printed devices have shown a high shape-memory function.[29] In a recently published studies, researchers have synthesized and 4D-printed methacrylate polycaprolactone precursor polymers using a UV-light-emitting-diode SLA printer based on magnetic resonance imaging (MRI) data. The 4D printed stent accurately matched the tracheobronchial structure and cartilaginous rings with reduced migrations. Furthermore, the low profile of the SMP stent also made it easier and less injurious in stent deployment.[30] The 4D bioprinting strategy is based on the integration of shape-memory biomaterials and 3D bioprinting technology for the production of transformative polymer-cell bioconstructs.[30] This innovative technology is now expected to be used in areas such as tissue engineering, regenerative medicine, bioelectronics, and personalized medical devices.

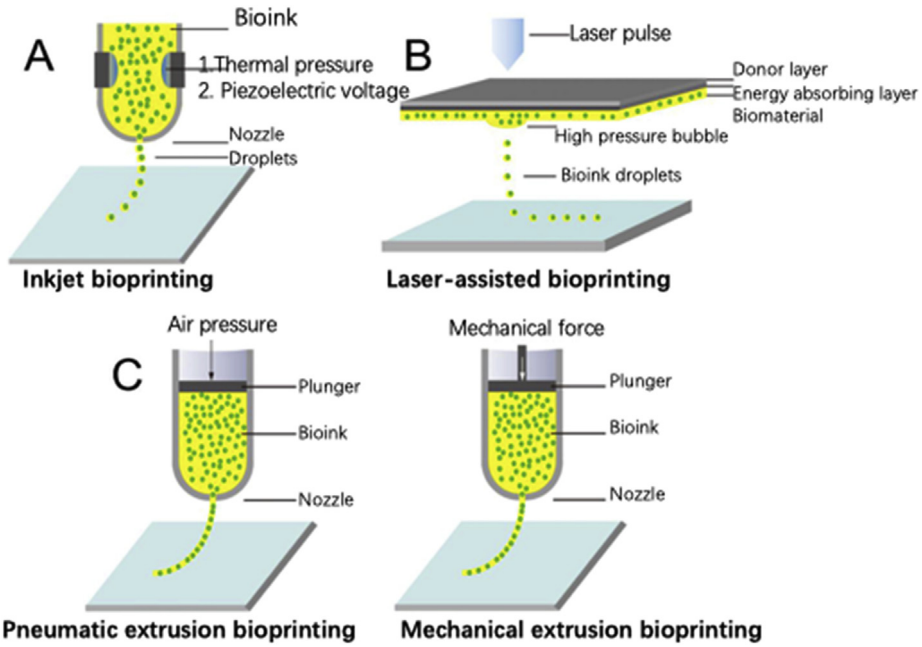

Fig. 4. Illustrations of three mainstay bioprinting techniques. (A) IBP. (B) Laser-assisted bioprinting. (C) Extrusion bioprinting.[26]

3DP technologies in interventional radiology

3DP technologies have been used for many years in the clinic, especially in designing patient-specific devices and anatomical models based on CT and MRI data. Currently, 3DP can be used in interventional radiology for preprocedural planning, medical device production, and medical research. At present, the cost of printing personalized medical implants, such as stents, via SLS EBM technologies is significantly higher than that of mass-produced ones. However, meta-analyses have shown that the use of customized devices could significantly increase surgical accuracy, reduce procedural/radiation exposure time, improve the outcome of the surgery, and reduce hospital stay time. Nevertheless, more evidence and long-term follow-up data are required to determine if the use of 3D-printed devices could become routine clinical practice. In the following sections, we discuss the recent clinical applications of 3DP in interventional therapy.

Neurointervention

3DP can recapitulate the brain vascular system using angiography data and validate procedural manipulation in vitro. Furthermore, 3DP has been used in research and patient education for providing models with patient-specific anatomy (Fig. 5).[31] A 3DP replica was shown to be an anatomically precise model, and many of them were fabricated using ABS (Fig. 6).[32]

Intracranial aneurysms

Intracranial aneurysms (IAs) are accompanied by the risk of catastrophic rupture. Nowadays, an increasing number of interventionalists are using 3DP in brain aneurysm treatment.[33] Frölich et al. used 3DP to produce hollow aneurysm models, thus replicating a wide range of aneurysm geometries and sizes. The authors observed a high level of anatomical accuracy in the models with a mean Dice index of 93.6 ± 2.4% as compared with the angiography data. They highlighted that more research is required to create aneurysm models with realistic texture. If coils and other implants could be placed in 3DP models in a manner similar to arteries, experiments could be performed on neurointerventional devices in vitro to replace the use of animals.[34] Similarly, Anderson et al. also showed that aneurysm diameter measurements of the 3D printed models correlated well with the source images ($r = 0.999$; $p < 0.001$), with no statistically significant group difference ($p = 0.4$). 3D printed models could be produced in-hospital and on-demand. These models can be used for flow studies with computational fluid dynamics.[35] Kim et al. used aneurysm models to educate patients and obtain informed consent from them, and the use of the 3D model was associated with a higher understanding and satisfaction of preoperative patient consultation as compared with conventional counseling.[36]

Coiling is the mainstay of IA treatment. Appropriate microcatheter shaping is crucial for the stable embolization of IAs and affects the packing density of the coil. There are many publications on 3DP-aided microcatheter shaping. In 2015, Namba et al. reported using 3DP models to optimize microcatheter shaping to improve microcatheter accuracy and stability during IA treatment. The microcatheter was preshaped and validated prior to the procedure using the 3DP model. Ten consecutive IAs were coiled using this method, and nine of the preplanned microcatheters demonstrated stability during embolization (Fig. 7).[37] Xu et al. reported another application of 3DP in microcatheter shaping for IAs. The authors selected the best-shaped microcatheter tips using a 3D software, printed the tips using 3D printers, and then compared them with real microcatheters before the coil embolization. The use of this method enhanced the accuracy and stability of the microcatheter position during the procedure. A total of 13 patients were enrolled in the study, no complications such as an aneurysm rupture occurred, and the catheter tip position remained stable. All the aneurysms were densely coiled in the report (Fig. 8).[38] Another team used 3DP in a different manner for microcatheter shaping. The microcatheter was placed in the target position of a cerebral vascular model and immersed in hot water for 5 min for the shaping. The shaped microcatheter was then sterilized and directly used for brain aneurysm embolization. It was found that the new shaping method used for embolization was safe and efficient.[39]

For device testing, Xie et al..[40] first introduced the usage of rapid prototyping in 2009. They developed a neurovascular model with a sinuous shape mimicking the human intracranial carotid artery (ICA). The curved vessel model was established with the help of a 3D-printed silicon tube based on MRI data of a human ICA. The navigability and device performance of intracranial stents were successfully tested with

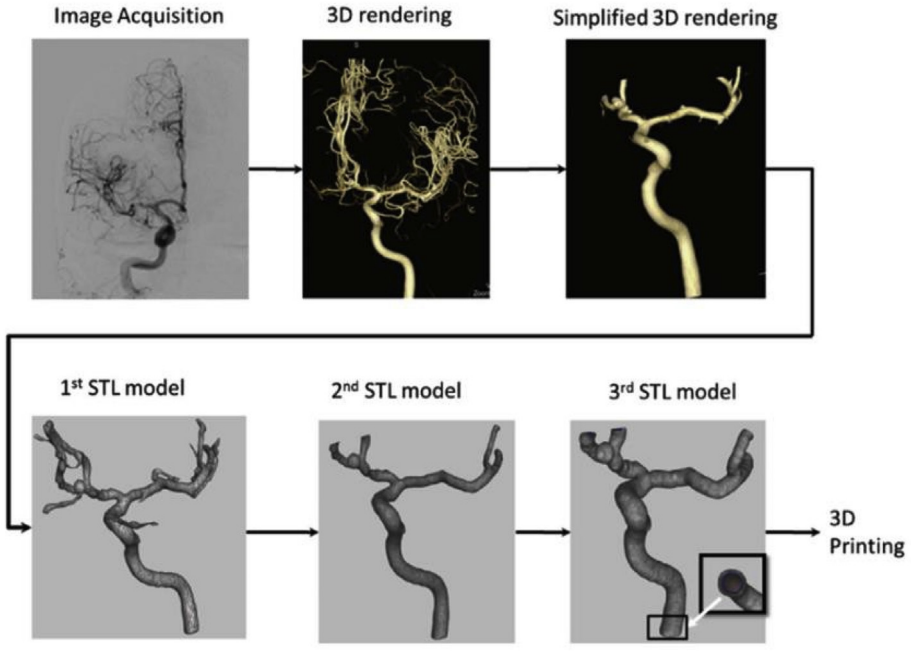

Fig. 5. Preparation steps for 3DP.[32]

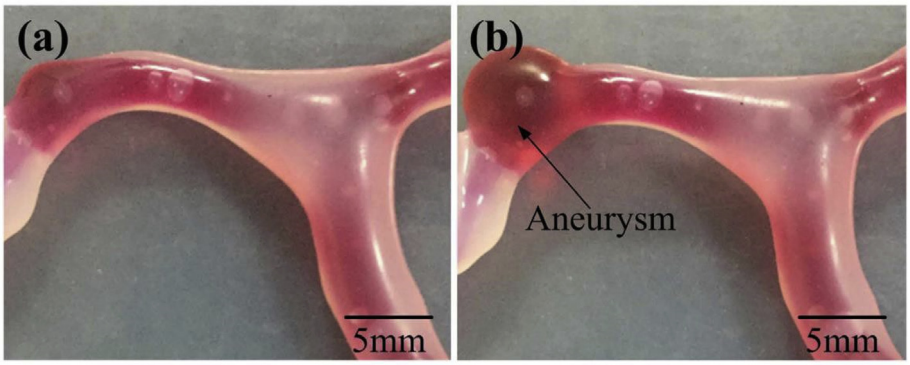

Fig. 6. Comparison of the brain vascular model. (a) No blister-like dilation bulges in the vascular model; (b) presence of a blister-like aneurysm.[32]

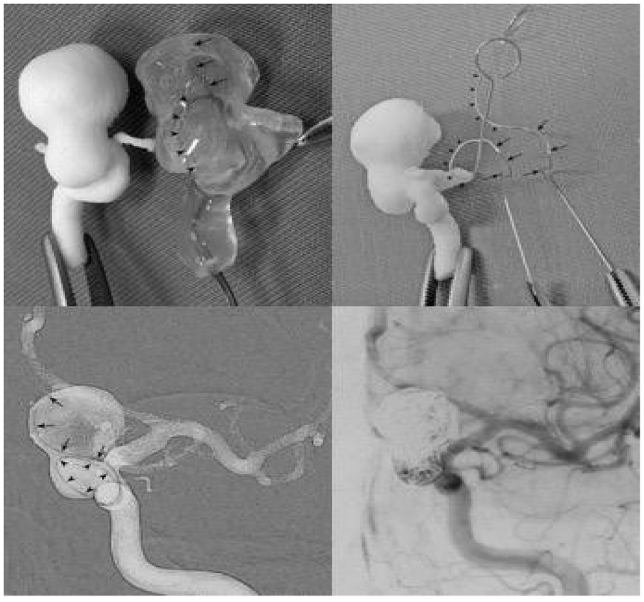

Fig. 7. Pre-planning of the shaping mandrel of microcatheter using 3DP rapid prototyping technology.[37]

this model. They opine that their method has high controllability, repeatability, and factuality, and 3DP is also useful for training the neuroradiologists and interventional physicians. 3D neurovascular models have also been used to directly test the navigability of catheters in vitro in different tortuous anatomies and positions and for devices such as optical coherence tomography lenses and flow diverters (Fig. 9).[41] In basic research, Kaneko et al. cocultured and coated a patient-specific IA model with endothelium; they used the endothelialized model to study the biological effect of a complex-flow stress on the endothelial cells.[42]

A 3DP vascular model has also been used to simulate the process of a cerebral aneurysm formation and to familiarize the neurosurgical clinician with patient-specific anatomy of cranial nerves, the brain, vessel branches, and the skull at a low cost (approximately USD 25 per replica).[32]

Brain arteriovenous malformation

Brain arteriovenous malformation (bAVM) treatment requires detailed information regarding the anatomical and lesion structure. Although it is difficult to reconstruct bAVM models as the structure of the lesion is often complicated, Shah et al. reported successful 3DP of a complex bAVM for preoperative investigation. All the models depicted the course, size, and number of feeding vessels and draining veins, as well as the relationship of the nidus with the brain. Using this model, it was possible to identify the normal and abnormal vessel architectures

Fig. 8. Application of 3DP in selecting the best-shaped microcatheter tips using a 3D software, and the tips were printed using 3D printers. Using this method, it was possible to enhance the accuracy and stability of the microcatheter position during embolization.[38]

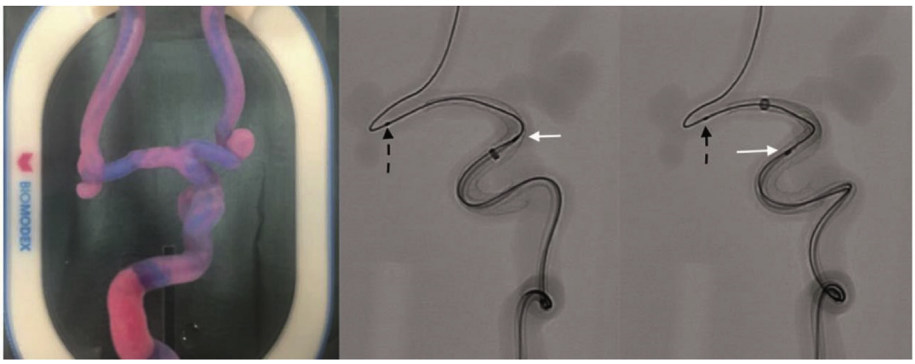

Fig. 9. Surgical simulation of flow diverting treatment of intracranial anterior circulation aneurysm with 3DP silicone replica. White arrows indicate pipeline shield and black dashed arrows indicate the microwire.[41]

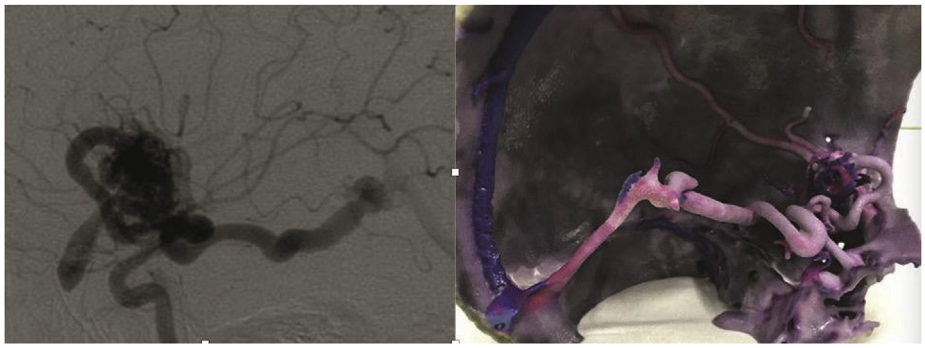

Fig. 10. (a) A case of a 21-year old male patient with Sylvian fissure bAVM (b) and printed 3D model showing the nidus and the arterial feeders and the draining veins.[43]

(Fig. 10).[43] Similarly, Dong et al. used bAVM models as an educational and clinical tool for patients, doctors, and surgical residents. The whole printing process was completed "in-house" using CT angiography (CTA) or digital substraction angiography (DSA) data. Intraoperative validation of the model fidelity based on DSA images of the same patient showed that the printed models precisely replicated the actual bAVM structure with a mean variation of less than 2 mm. The authors emphasized that the solid model—other than digital 3D images—of the lesion and surrounding anatomy may potentially reduce operative time and surgical risks. The FDM technology of 3DP can be fast, accurate, and cost-effective

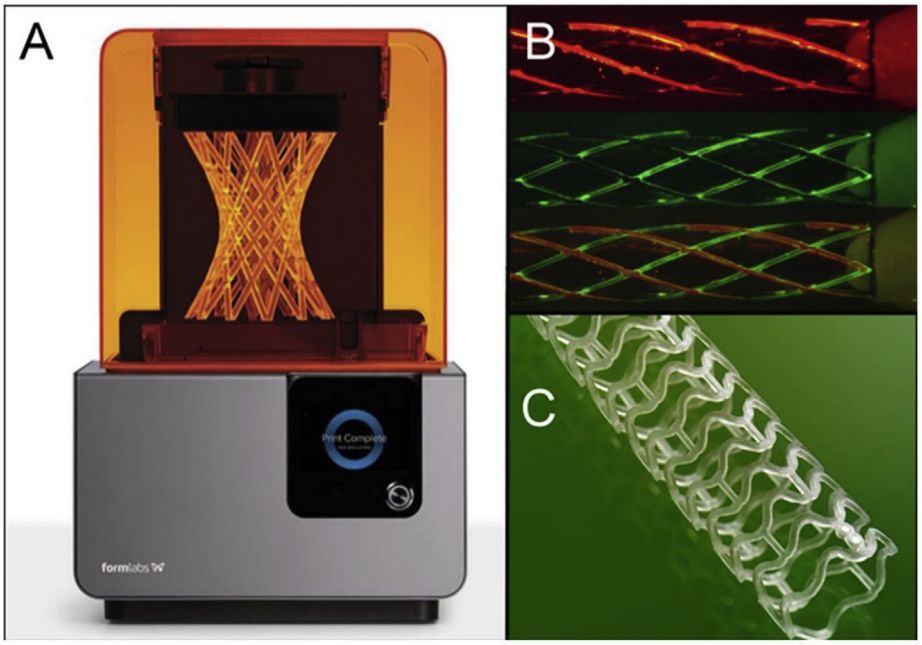

Fig. 11. (A) Liquid-based 3D printers using laser to harden resin to create 3D structure (Courtesy: Formlab© 2015, Somerville, MA). (B) Prototype stents can be printed using different materials including metal (indicated by different colors). (C) A PLA bioabsorbable 3DP stent that is commercially available.[48]

in bAVM-model fabrication.[44]

Acute ischemic stroke

Thrombosis in acute ischemic stroke patients involves factors including the blood, vessel wall, vessel geometry, and flow patterns. Costa et al..[45] were able to reproduce the 3D geometry and blood-flow patterns of stenotic blood vessels by applying SLA 3DP. They produced a proof-of-principle miniaturized artery of patient-specific geometries with endothelialized microfluidic chips in it to study the impact of vessel morphology and blood flow patterns on platelets in arterial thrombosis.

3DP in cardiovascular intervention

Cardiovascular disease is among the leading causes of mortality worldwide and causes approximately 20 million deaths annually.[46] Millions of heart vascular implantations are performed globally every year. Cardiovascular applications of 3DP technology include patient-specific models for the evaluation of heart valve and vessel function, procedural planning, medical teaching, and development of new percutaneous devices (Fig. 11).[47,48]

Percutaneous coronary intervention (PCI)

Stenting is a common revascularization strategy in PCI for treating coronary artery stenosis.

However, patients generally receive metal stents without an individualized design. Current stents used in the clinic are only available in certain sizes, and stents of the same lengths may not achieve the same effectiveness in different arteries. Therefore, personalized stents for accurately measured lesions may be necessary in improving the outcomes of such treatments.[48] Misra et al. first introduced a prototype of a personalized stent fabricated using 3DP to reduce the restenosis in a pig coronary artery model. They suggested the feasibility of using 3D printed biodegradable stents in real patients after necessary improvements.[49] A 4D-printed, thermo-responsive, shape-memory cardiovascular stent was fabricated by Ge et al. and on heating it, the stent was able to recover its original larger diameter, which was used to dilate the narrowed artery.[50]

In-stent restenosis is a critical issue after coronary interventions. Wang et al..[51] described a method of decreasing restenosis via optimal stent positioning based on a 3DP model. They placed real stents inside patient-specific microfluidic coronary models, studied hemodynamic changes after stenting, and suggested that by studying the hemodynamic results of the 3DP models, the best stenting strategies could be identified to maximally reduce restenosis. 3DP was also used in the interventional planning and device sizing for coronary fistulae.[52]

Congenital cardiovascular diseases and valvular disorder

Congenital cardiovascular diseases are often complex and comprise distinct geometries. It can be very difficult to completely understand some diseases, such as tetralogy of Fallot and hypoplastic left heart syndrome, using current imaging modalities.[53] 3DP heart models have been used for enhanced structural orientation, patient-specific hemodynamic evaluations, pre-procedural planning, aiding ventricular device placement, and testing novel strategies.[54] Testing devices of various sizes and designs in 3DP models may aid in reducing shape/size mismatches between interventional devices and surrounding structures. 3DP has also been applied in treating valvular disorders by fabricating the mitral, aortic, and pulmonic valves in order to select optimal devices for reducing complications such as paravalvular regurgitation, device failure, or ventricular outflow tract obstruction (Fig. 12).[47,55] Vukicevic used deformable 3D models to evaluate the deformation of the surrounding structures (e.g., vessel wall, chamber wall, and valve leaflet) caused by the implanted TMVR (transcatheter mitral valve repair) device before surgery, thus assisting in the optimization of TMVR approaches. They also found that texturized 3D modeling could be invaluable in studying the impact of valvular calcification on device landing and in simulating patient-specific valve function.[56]

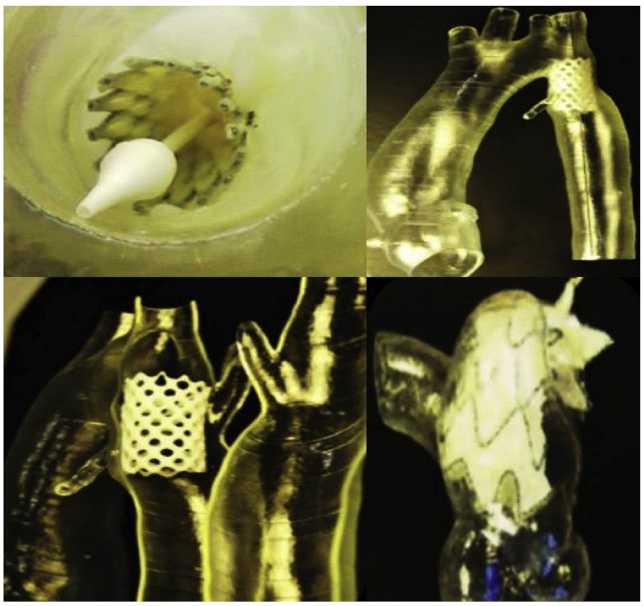

Fig. 12. Transcatheter aortic procedure performed within an aortic stenosis model.[47]

Pre-TAVR (transcatheter aortic valve replacement) 3DP based on cardiac imaging data has been used to evaluate the interaction between the aortic root and implanted valves. In addition, 3DP was also applied using flexible materials to replicate calcified, stenotic aortic valves with leaflet movement to improve patient-specific TAVR planning.[57] Qian et al. used 3D printed phantoms for performing an in vitro simulation before performing a TAVR. The system could aid in predicting the occurrence, severity, and location of post-TAVR paravalvular leaks.[58] The use of a 3D-printed right ventricular outflow tract in intervention planning and device selection for treating percutaneous pulmonary valve stenting dates back to 2007.[59]

Aortic aneurysms

Aortic aneurysm (AA) patients may lose their lives immediately after aneurysmal ruptures. The first introduction of the endovascular AA repair (EVAR) in 1990 provided a mini-invasive method to replace open surgery. However, for lesions with complex neck anatomies or lesions close to main arteries, EVAR remains challenging. AA models can be manufactured using 3DP technology. A hospital center reported using a 3DP simulation model to overcome the difficulties in performing EVAR. They performed a simulation using AA models before the endovascular intervention to visualize the guidewire manipulation and determine the optimal stent placement.[60] In 2013, Tam et al. described a printed aneurysm with complex neck anatomy to facilitate the visualization of the neck anatomy and EVAR surgery.[61] Recently, Torres developed an EVAR simulation system using 3DP aneurysms and found that patient-specific training prior to EVAR reduced fluoroscopy time, surgery time, and the volume of contrast used during the procedure (Fig. 13).[18] Meanwhile, a fenestrated endograft is often used in treating abdominal AAs. However, it is challenging to construct one for complex cases, and inaccurate positioning of the endografts may influence vessel branch patency and reintervention. 3DP models have been used to guide physician-modified endograft planning (Figs. 14 and 15).[62,63] Taher et al. constructed patients' aorta models to allow the physician to pre-implant the devices and to review their fitness. They showed that one in five endografts (22%) were required to be modified before implantation. This

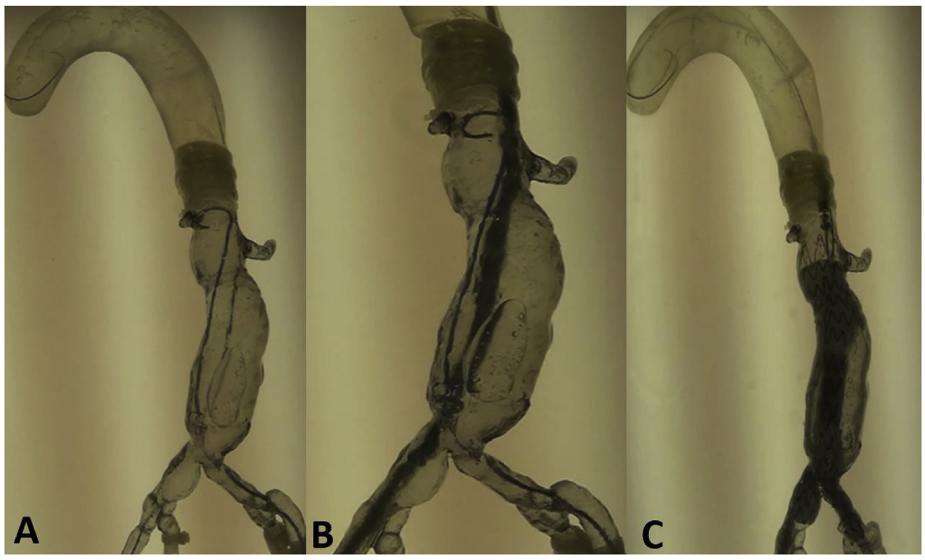

Fig. 13. EVAR steps simulated in a 3D model. (A) Guidewire and catheter in position. (B) Main body of the stent graft in position. (C) Stent graft deployed.[18]

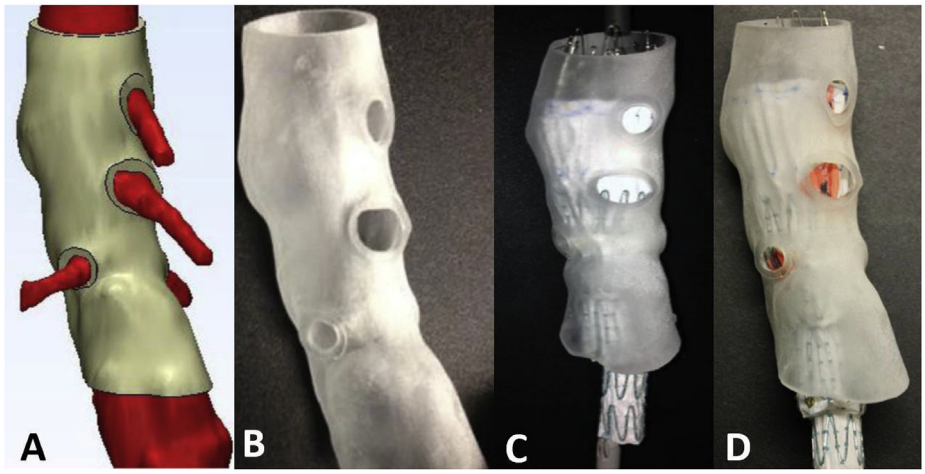

Fig. 14. Process of determining fenestration locations on endograft. (A) Fenestration model created by computer software. (B) 3D printed fenestration model. (C) Stent graft is deployed inside the model. (D) Fenestration locations are marked onto the graft through the holes of the fenestration model.[62]

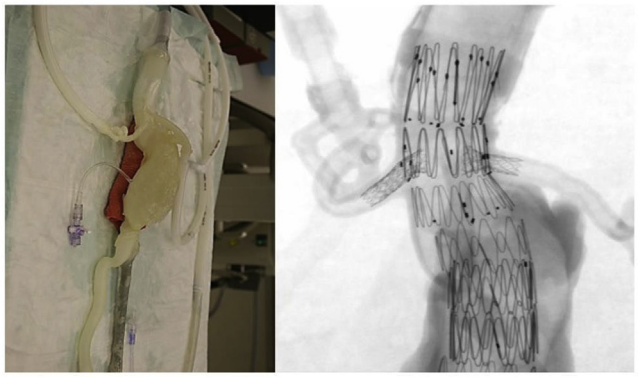

Fig. 15. Picture of 3D-printed AAA model (left) and its fluoroscopic image during the simulation (right).[63]

highlighted the potential of 3DP in avoiding adverse EVAR events associated with mismatched fenestrations and branch blocking.[64] Rynio et al. developed a 3D-printed template of the aortic arch to assist the

Figure 16. (A) 3DP model of the aortic arch. (B) Preparation of stent graft fenestration in the 3DP model.[65]

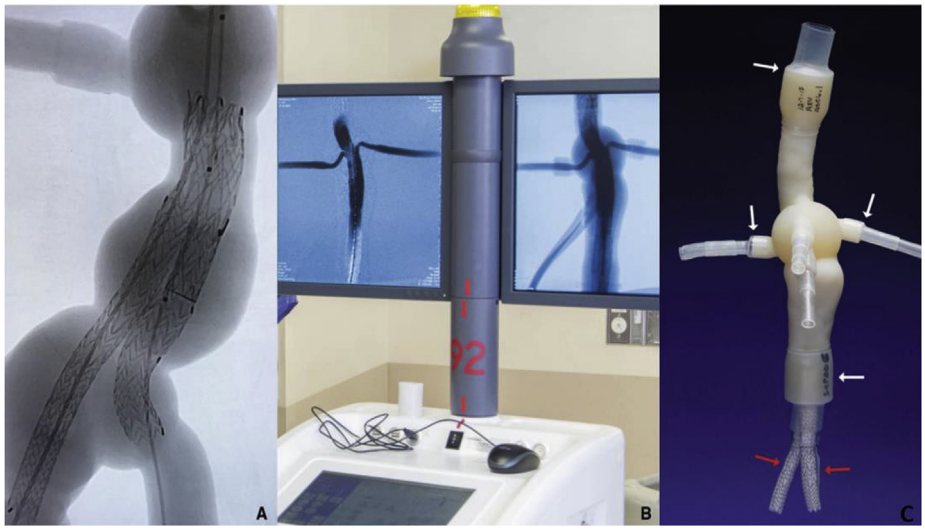

Fig. 17. Fluoroscopy images (A) and EVAR simulation result (B) of 3D-printed AAA model with the attachment of plastic/silicone tubes connected to a fluid pump with water flow (C).[66]

fenestration and modification of the stent-graft. This is the first case report on the use of 3DP in accurate stent deployment for the endovascular repair of a descending thoracic aneurysm (Fig. 16).[65] Kärkkäinen simulated EVAR using a printed AAA (abdominal aortic aneurysm) model connected to a hemodynamic pump. The AAA model was fabricated using the Objet500 Connex3 (Stratasys, Eden Prairie, MN) printer. A total of 22 EVAR simulation procedures were performed with a mean procedure time of 37 ± 12 min. The authors simulated all the procedural steps with high fidelity. This method may be applied to endovascular skill training (Fig. 17).[66]

Aortic dissection aneurysms have also been 3D printed to better visualize the details of the dissection (size, branches, and true/false lumens); the mean luminal diameter difference between the printed model and CT images were less than 0.5 mm. This could allow clinicians to conduct a preoperative simulation of endovascular stent grafting procedures confidently.[67]

Several review papers have highlighted the merits of 3DP in the cardiovascular field, which include the reduction in procedural complications, time required, and costs and enhanced precision of cardiovascular interventions, improvement in physician-patient communication, and as a training opportunity for interventionists.[68]

3DP in peripheral vascular intervention

The use of degradable stents may result in fewer rejection reactions and less damage to vessel walls as compared with that in the case of metal stents. PLA or PCL vascular stents manufactured using FDM technology are common.

Peripheral vascular stents

Wu et al. evaluated the self-expanding parameters of a shape-memory PLA stent. They showed that, at a recovery temperature of 65 °C, the diameter recovery ratio of the PLA stent was excellent (between 95% and 98%), and the length recovery ratio was greater than 97%. Although the transition temperature of the PLA is higher than the human-body temperature, the feasibility of self-expansion of the 3D printed PLA vascular stents was proven.[69] Guerra et al. produced a smaller PCL/PLA composite stent using a novel 3D tubular printer based on FDM and demonstrated the abilities of the stents in inducing rapid reendothelialization and fulfilling mechanical requirements. Their 3DP process could produce composite stents with an accuracy as high as 95%. The PCL and PLA stents reached a cell proliferation of 12.46% and 8.28%, respectively, within 3 days. Furthermore, the composite stents (PLA/PCA) could improve the mechanical properties of materials. Moreover, the smaller the cell area of a stent, the better the cell proliferation rate. PCL showed a better degradation rate than PLA (Figs. 18 and 19).[70]

Tumor intervention

3DP has also been applied in tumor intervention. It has been shown that 3DP is a feasible technology that may facilitate procedural practice and aid in achieving superior clinical outcomes. 3DP has been used to visualize anatomic relationships among the hepatic arteries, portal veins, bile duct, and liver tumor (Fig. 20).[71] A recent study has presented data regarding 3D renal tumor printing, which represents the first model used for anatomical visualization of arteries, collecting system, and the tumor

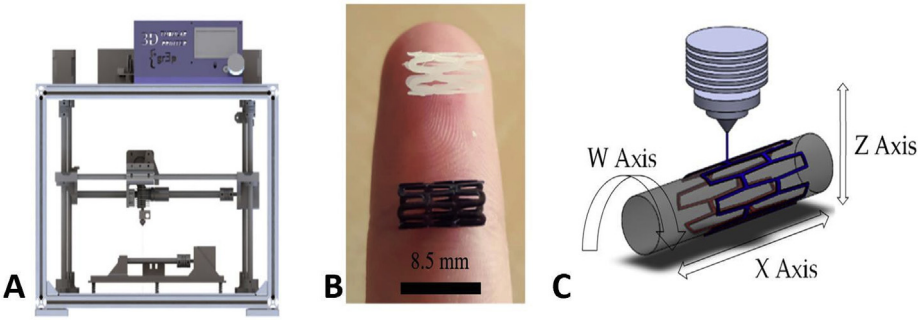

Fig. 18. 3D tubular printer (A) 3D-printed stents [PCL in white, PLA in black] (B), and printing methodology (C).[70]

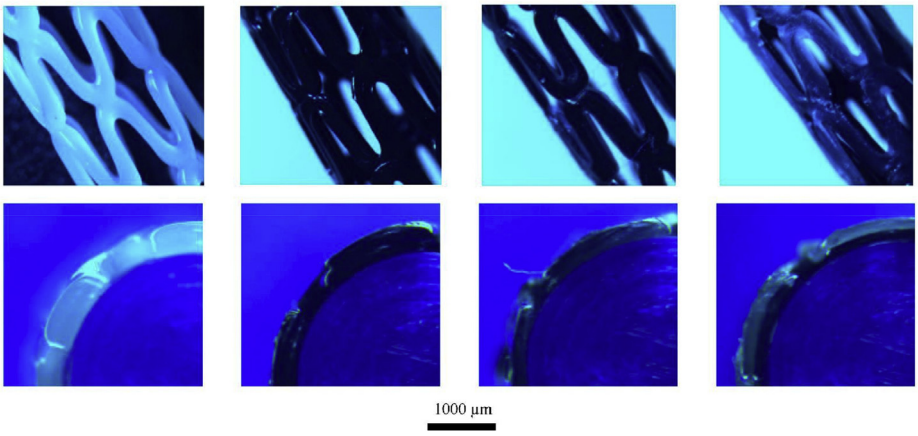

Fig. 19. Optical microscope images of 3D-printed stents. The top row of images shows the general view, and the bottom row of images depicts the sectional view.[70]

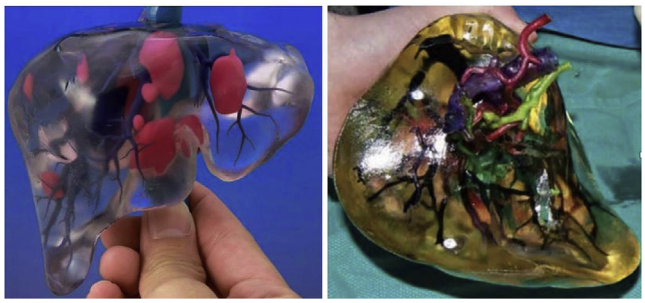

Fig. 20. 3D-printed liver cancer model. Different colors indicate blood vessels, biliary tract, and tumors.[71]

itself. The 3D tumor printing provided an accurate anatomical representation for patient education and procedural practice with realistic simulation.[72]

Visceral aneurysms

Shibata et al. tested the accuracy of hollow 3DP models of visceral aneurysms based on the CTA data of 19 patients. They found that the sizes and shapes of the printed models have no significant difference from the imaging data ($P = 0.56$). The most accurate model exhibited a difference of only 2 mm^3 (0.05%). They concluded that these models could be used for endovascular treatment simulations.[73] Similarly, Takao et al. used an FDM-type 3D printer to fabricate an a splenic artery aneurysm for the simulation of endovascular treatment. They found that, as the material used for the model production, ABS is more flexible and PLA is more solid, while but nylon is both strong and flexible.[74] Itagaki reported on small-caliber vascular models used for endoluminal testing of devices. Before the endovascular treatment of splenic artery aneurysms, a 3D printed model was used to test the catheter positioning and practice the procedure. They identified the best guiding catheter and microcatheter during testing and finally used the combination in embolization successfully. They concluded that 3DP vascular models are useful in procedural planning and intraoperative guidance. A complex endovascular procedure could be practiced and refined using 3DP preoperatively.[75]

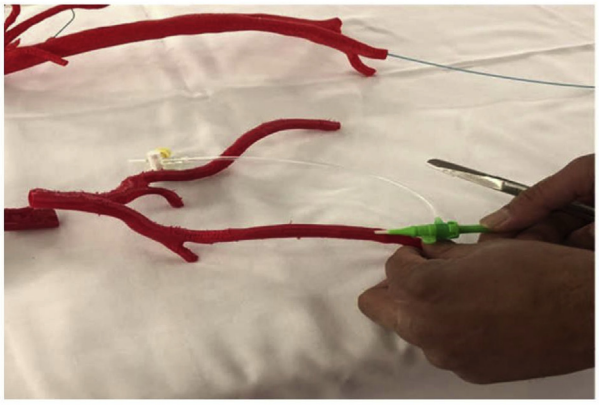

Fig. 21. Peripheral real-size vasculature from a CT angiogram and printed using red PLA.[78]

Others

3DP has also been applied in the Budd–Chiari syndrome (BCS). Nai et al. printed a patient-specific 1:1 BCS inferior vena cava model using MRA data. The architecture features of the inferior vena cava and the hepatic veins were successfully reproduced, and the authors simulated the interventional manipulation before the operation to select an appropriate balloon and stent. This BCS model was very helpful in guiding procedures and improving physicians' and patients' understanding of the disease.[76] Percutaneous pulmonary interventions require extensive navigation of the catheter and guidewire. In a recent study, Witowski et al. demonstrated that 3DP-assisted balloon pulmonary angioplasty for chronic thromboembolic pulmonary hypertension and 3DP-assisted stenting for pulmonary artery stenosis were feasible. Personalized real-size models printed prior to the surgery provided additional tactile experience with straightforward manipulation, and the 3D visualization techniques have potential for reducing the dosage of contrast medium and thus minimizing the risk of acute kidney injury.[77] 3DP can also be used to produce models for femoral vessel access puncture training, thus improving the surgeon's performance and self-confidence (Fig. 21).[78]

Non-vascular intervention

Airway obstruction (CAO)

3DP has been adopted by interventional radiologists in central airway obstruction (CAO) stenting to avoid tissue ingrowth and device migration, which were commonly observed in conventional stents. Zarek et al. 4D-printed a shape memory (semicrystalline methacrylated polycaprolactone) tracheal stent based on the patients' imaging data; the stent could prevent migrations better. After being inserted, the tracheal stent could expand to the permanent shape at a temperature matching that of the patients' anatomy (Fig. 22).[30]

3DP implants have also been used in newborns in the case of airway

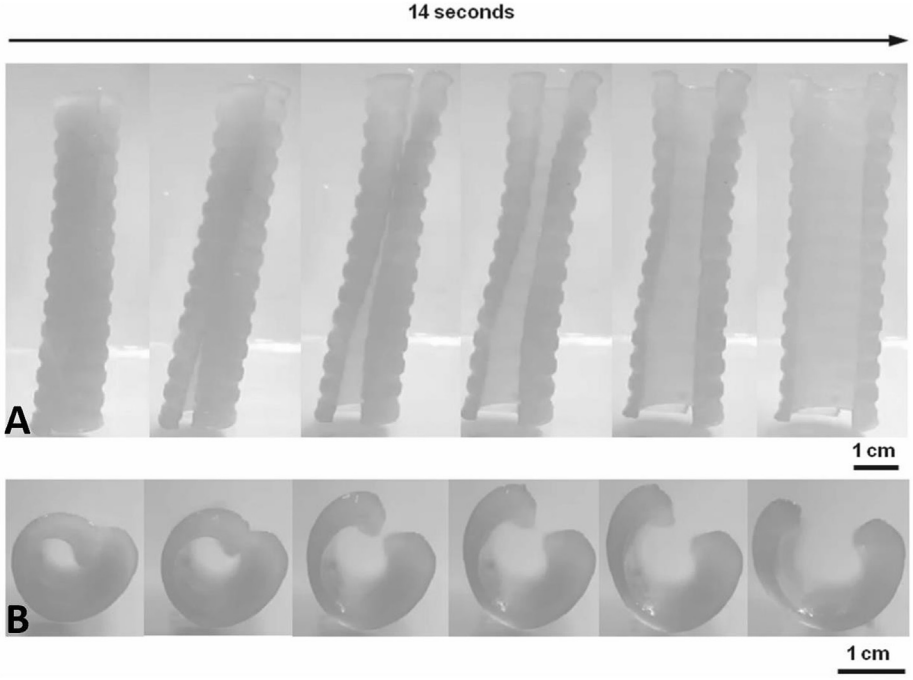

Fig. 22. 3DP personalized airway stent. (A) Images show the transition between the temporary state (for deployment) and the permanent shape (for performance). (B) Axial view of the process.[30]

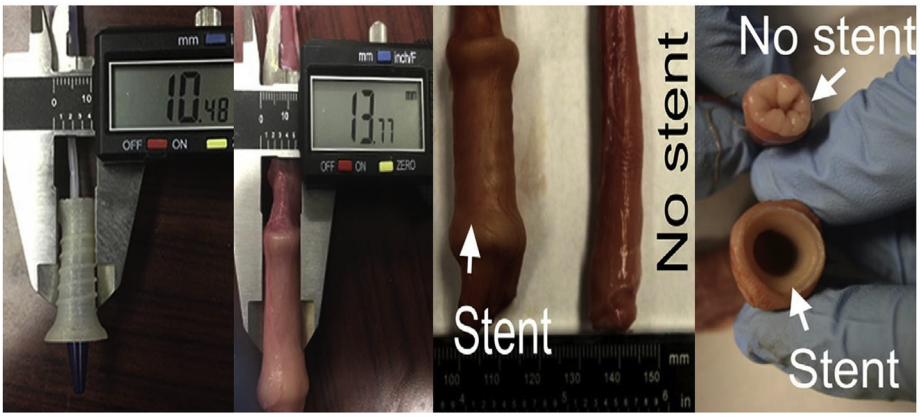

Fig. 23. 3DP esophagus stent and released state in the esophagus.[85]

collapse. Because the infant airway is under rapid growth, the application of standard stents is not feasible. To overcome this, Zopf et al. developed a custom bioresorbable tracheal splint for a child with tracheobronchomalacia, and the device successfully decreased the venous carbon dioxide pressure. The child was cut off from ventilation support and discharged without complications.[79] This approach was also successful in three other pediatric patients with tracheomalacia.[80] In the case of adults, Guibert et al. treated a post-transplant CAO using a fully customized silicone airway stent fabricated using 3DP.[81] Young et al. used 3DP-customized silicone stents for treating complex airway stenoses caused by granulomatosis polyangiitis in two patients, which resulted in durable improvements. The stents could remain in place for 5–8 months.[82] 3DP has also been used to guide impassable procedures. Guibert et al. reported choosing an appropriate stent and guiding the stent insertion for impassable inflammatory tracheal stenosis based on a printed model of the trachea.[83] For tracheal repairment, Jung et al. developed a 3DP biomimetic tracheal prosthesis, which could support a tracheal defect and allow the host tissue to heal in a rabbit model.[84]

Gastroenteric diseases

Complications such as tissue ingrowth and stent migration may be encountered when treating dysphagia with esophageal stents in inoperable patients. Lin et al. recently printed a flexible polymer stent with anti-migration spirals. Ex vivo experiments in a porcine esophagus showed that the degradable stent with spirals significantly lowered the migration distance compared to control stents without spirals. Degradation took place 6 weeks after the implantation, and the mechanical prosperities did not considerably change until after 3 months (Figs. 23 and 24).[85]

Interestingly, a team collaborated with Mayo Clinic and bioprinted a novel polyvinyl alcohol biliary stent with a stem cell-collagen-cholangiocyte coating. This approach may allow the interventionalist to fabricate personalized bio-integrating stents for use in biliary procedures. It may pave the way for the translation of bioprinted stents from bench to bedside in the field of bile duct obstructions.[86] Furthermore, stomach models were printed for endoscopic training, and the 3DP simulator realistically reflected endoscopic handling and was proven useful in improving the operative skills of trainee endoscopists

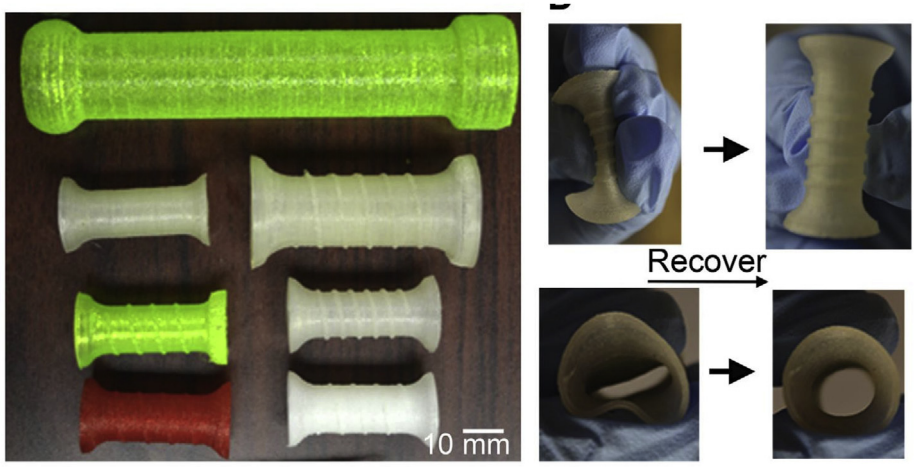

Fig. 24. Different types of 3DP esophagus stents of different structures and materials (left). The stent was compressed and then recovered to the original shape (right).[85]

Fig. 25. (A) Upper gastrointestinal tract prototype STL file. (B). 3D-printed silicone moldings. (C) Assembled silicone moldings.[87]

(Fig. 25).[87]

Iodine-125 (^{125}I) brachytherapy

Radioactive Iodine-125 (^{125}I) brachytherapy is safe and effective in treating many tumors, including cancers of the head, neck, lungs, pancreas, rectum, prostates, and recurrent/metastatic lesions. Because the dose rate of ^{125}I seeds declines rapidly in tissue, precise implantation is a requisite for treatment efficacy. In recent publications, some researchers used rapid prototyping to design guiding templates to assist the implantation of ^{125}I seeds into tumors. Pan et al. reported patient-specific coplanar templates fabricated with a 3D printer to improve the accuracy and safety of CT-guided ^{125}I implantation in 30 patients with malignant tumors. Eighty percent.

(24/30) of the patients achieved excellent dosimetry results (90% dose of target volume and 100% target volume of prescription dose), and five patients (16.7%, 5/30) achieved good dosimetry results. The technique provided a satisfactory quality of implantation with less procedure-related short-term adverse events.[88] In the article by Liang et al. the 3D-printed template was also confirmed to be reliable in guiding ^{125}I seeds implantation for the treatment of lymph node metastasis. All the operations were successfully completed. The quality of ^{125}I seed implantation was excellent, good, moderate, and poor in 11, 3, 1, and 0 patients, respectively. No severe complications occurred.[89]

Owing to the location of the pancreas and its complex anatomical relationship, complications associated with Iodine-125 brachytherapy in patients with pancreatic cancer are common.[90] A group found that 3D-printed coplanar templates were useful in guiding ^{125}I seeds implantation for pancreatic cancer. Their 3D coplanar template was designed and produced using preoperative CT data. Percutaneous puncture and ^{125}I seed placement were realized in all ten patients with only one minor complication. The postoperative dosimetry parameters were consistent with the preoperative planning in all cases ($P > 0.05$).

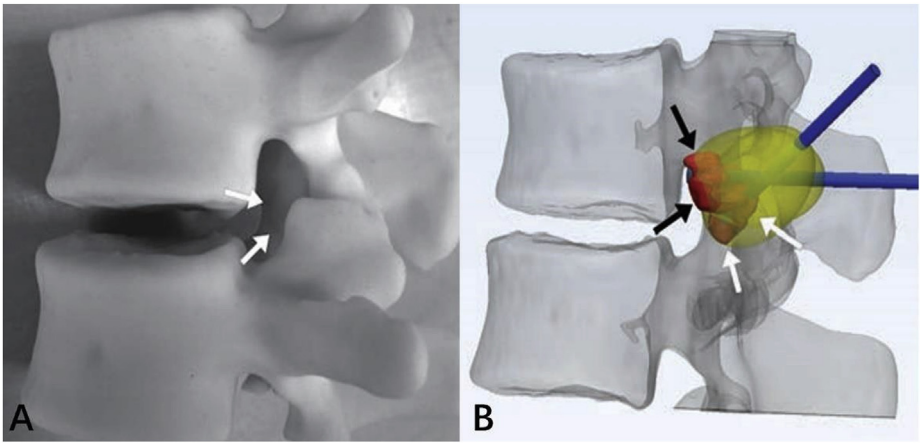

Fig. 26. 3D-printed model of L1 osteoblastoma; arrows indicate inferior palpable tumor lobule (A). (B) Advanced 3D visualization displays cryoprobe tracts (blue) used during the model simulation and theoretic ablation zones (yellow). Red indicates the tumor lobules.[92] (For interpretation of the references to color in this figure legend, the reader is referred to the Web version of this article.)

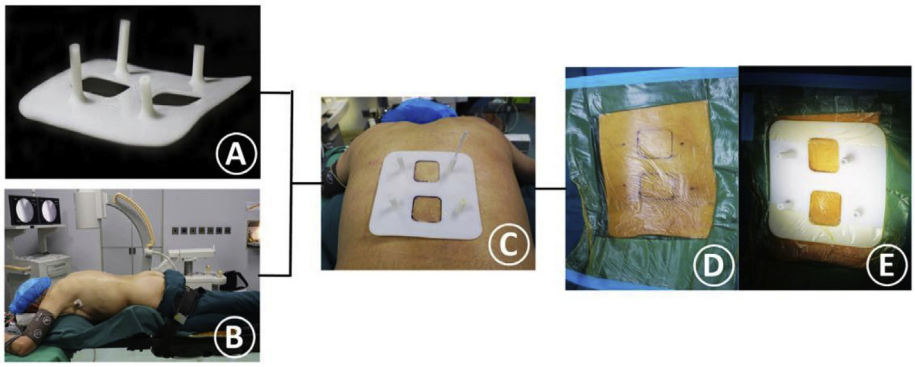

Fig. 27. (A) 3D-printed guiding template for precise PVP. (B) Patient's intraoperative position. (C) Matching the two location holes. (D) Marking the skin entry points and disinfect the surgery area. (E) Fixing the sterile guide template on the back skin.[93]

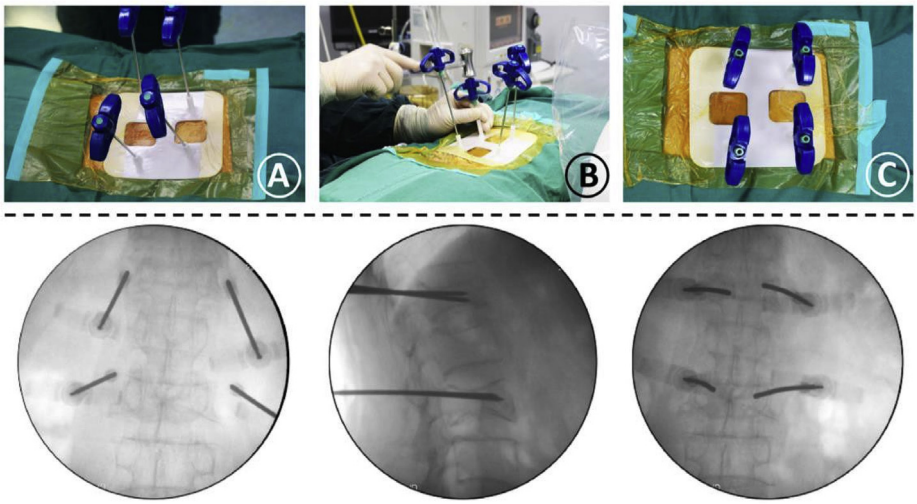

Fig. 28. (A) Confirmation of the needles' location. (B) The needles were gradually inserted into pedicles along the guiding cylinders. (C) The needles were completely inserted into the guiding cylinders of the template, and its final location was observed in the fluoroscopic images.[93]

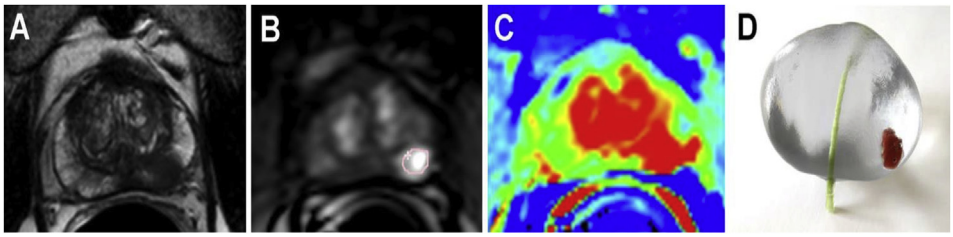

Fig. 29. (A–C) Multiparametric MRI prostate transverse view. (D) 3D-printed model of a patient-specific prostate with tumor structure (red) and urethra (green).[96] (For interpretation of the references to color in this figure legend, the reader is referred to the Web version of this article.)

They suggested that a 3D-printed template is helpful for realizing the precise implantation of ^{125}I seeds in treating pancreatic cancer.[91]

Vertebral tumors

Percutaneous image-guided ablation of vertebral tumors is challenging because of the presence of adjacent crucial structures such as nerve roots and the spinal cord. Spinal injuries and cerebrospinal fluid leaks have been reported after these procedures. For improving the procedural safety and efficacy, 3DP has been used for the procedural planning of MRI-guided cervical and lumbar tumor cryoablation in complex cases (Fig. 26).[92]

Similarly, 3DP has been adopted to reduce puncture-related complications in percutaneous vertebroplasty (PVP) treatment of vertebral compression fracture. Lia et al. used a 3D printed guiding template for realizing precise PVP. During the operation, by matching the guiding template to the patient's back skin, a stable needle orientation and accurate insertion were easily reestablished. On using this technique, the patient achieved even cement distribution without any procedural complications. Furthermore, the pain was relieved after the surgery (Figs. 27 and 28).[93]

Prostate cancer

Irreversible electroporation (IRE) is a novel treatment choice for prostate cancer (PCA), which has a high organ- and function-preserving

potential.[94] IRE uses microsecond electric pulses between two or more electrodes to generate nanopores in the cell membrane. These nanopores allow sodium/potassium/calcium to enter into or leave the cell. When above a certain threshold, the process could cause cell destruction owing to the ionic homeostasis disturbance.[95] However, a prostate with PCA is a very inhomogeneous tissue with hyperplasia, inflammation, cysts, calcification, urethra duct, and capsule; this makes prostate-specific IRE ablation planning challenging. Wendler et al. introduced a 3D bioprinted model for the simulation of IRE ablation to adjust the actual ablation field of the tumor and prostate before surgery. They bioprinted a prostate replica composed of matrices, cells, and possibly inorganic structures with a resulting heterogeneous structure based on patient-specific MRI data. This printed biomodel enabled pretreatment determination of the optimal individual IRE parameters (potential and electrode geometry) for an efficient PCA ablation (Fig. 29).[96]

Nevertheless, there are still several concerns regarding the regulations and standardization of 3DP applications in medicine. In May 2016, the FDA released a draft guidance on technical aspects for additive manufactured devices, including material controls, printing, and post-printing process, and assessment of the final devices for cleaning, sterility, and biocompatibility. Furthermore, there is still room for improvement in software, printing material, speed, precision, mechanical properties, and texture in 3DP. In addition, certain processing steps are time-consuming and expensive; it is necessary to modify 3DP workflows in terms of either the material design or by improving the printing technology to make it more efficient.[2,13]

In the near future, 3DP is expected to meet the needs of material diversity, realistic texture, and tissue/organ fabrication. It appears that as the clinical experience of 3DP utilization grows, 3DP can have an increasingly important role in patient-specific medicine and the development of interventional radiology.

References

1. Becker H. Hype, hope and hubris: the quest for the killer application in microfluidics. *Lab Chip*. 2009;9:2119–2122.
2. Liaw CY, Guvendiren M. Current and emerging applications of 3D printing in medicine. *Biofabrication*. 2017;9, 024102.
3. Waheed S, Cabot JM, Macdonald NP, et al. 3D printed microfluidic devices: enablers and barriers. *Lab Chip*. 2016;16:1993–2013.
4. Yin Chin S, Cheung Poh Y, Kohler AC, et al. Additive manufacturing of hydrogel-based materials for next-generation implantable medical devices. *Sci Robot*. 2017;2: eaah6451.
5. Krujatz F, Lode A, Seidel J, et al. Additive biotech-chances, challenges, and recent applications of additive manufacturing technologies in biotechnology. *N Biotech*. 2017;39:222–231.
6. Ho CM, Ng SH, Li KH, et al. 3D printed microfluidics for biological applications. *Lab Chip*. 2015;15:3627–3637.
7. Melchels FP, Feijen J, Grijpma DW. A poly(D,L-lactide) resin for the preparation of tissue engineering scaffolds by stereolithography. *Biomaterials*. 2009;30:3801–3809.
8. Xing JF, Zheng ML, Duan XM. Two-photon polymerization microfabrication of hydrogels: an advanced 3D printing technology for tissue engineering and drug delivery. *Chem Soc Rev*. 2015;44:5031–5039.
9. Shirazi SF, Gharehkhani S, Mehrali M, et al. A review on powder-based additive manufacturing for tissue engineering: selective laser sintering and inkjet 3D printing. *Sci Technol Adv Mater*. 2015;16, 033502.
10. Youssef A, Hollister SJ, Dalton PD. Additive manufacturing of polymer melts for implantable medical devices and scaffolds. *Biofabrication*. 2017;9, 012002.
11. Mazzoli A. Selective laser sintering in biomedical engineering. *Med Biol Eng Comput*. 2013;51:245–256.
12. Tappa K, Jammalamadaka U. Novel biomaterials used in medical 3D printing techniques. *J Funct Biomater*. 2018;9:17.
13. Ju Pucci, Christophe BR, Sisti JA, et al. Three-dimensional printing: technologies, applications, and limitations in neurosurgery. *Biotechnol Adv*. 2017;35:521–529.
14. Roh S, Parekh DP, Bharti B, et al. 3D printing by multiphase silicone/water capillary inks. *Adv Mater*. 2017;29:1701554.
15. Studart AR. Additive manufacturing of biologically inspired materials. *Chem Soc Rev*. 2016;45:359–376.
16. Compton BG, Lewis JA. 3D-printing of lightweight cellular composites. *Adv Mater*. 2014;26:5930–5935.
17. Kyobula M, Adedeji A, Alexander MR, et al. 3D inkjet printing of tablets exploiting bespoke complex geometries for controlled and tuneable drug release. *J Contr Release*. 2017;261:207–215.
18. Torres IO, De Luccia N. A simulator for training in endovascular aneurysm repair: the use of three dimensional printers. *Eur J Vasc Endovasc Surg*. 2017;54:247–253.
19. Lan Q, Chen A, Zhang T, et al. Development of 3D printed craniocerebral models for simulated neurosurgery. *World Neurosurg*. 2016;91:434–442.
20. Borovjagin AV, Ogle BM, Berry JL, et al. From microscale devices to 3D printing: advances in fabrication of 3d cardiovascular tissues. *Circ Res*. 2017;120:150–165.
21. Wilson Jr WC, Boland T. Cell and organ printing 1: protein and cell printers. *Anat Rec A Discov Mol Cell Evol Biol*. 2003;272:491–496.
22. Gudapati H, Dey M, Ozbolat I. A comprehensive review on droplet-based bioprinting, past, present and future. *Biomaterials*. 2016;102:20–42.
23. Skardal A, Mack D, Kapetanovic E, et al. Bioprinted amniotic fluid-derived stem cells accelerate healing of large skin wounds. *Stem Cells Transl Med*. 2012;1: 792–802.
24. de Ruijter M, Ribeiro A, Dokter I, et al. Simultaneous micropatterning of fibrous meshes and bioinks for the fabrication of living tissue constructs. *Adv Healthc Mater*. 2019;8, e1800418.
25. Nagarajan N, Dupret-Bories A, Karabulut E, et al. Enabling personalized implant and controllable biosystem development through 3D printing. *Biotechnol Adv*. 2018;36: 521–533.
26. Huang Y, Zhang XF, Gao G, et al. 3D bioprinting and the current applications in tissue engineering. *Biotechnol J*. 2017;12:1600734.
27. O'Brien CM, Holmes B, Faucett S, et al. Three-dimensional printing of nanomaterial scaffolds for complex tissue regeneration. *Tissue Eng B Rev*. 2015;21:103–114.
28. Lui YS, Sow WT, Tan LP, et al. 4D printing and stimuli-responsive materials in biomedical aspects. *Acta Biomater*. 2019;92:19–36.
29. Yang H, Leow WR, Wang T, et al. 3D printed photoresponsive devices based on shape memory composites. *Adv Mater*. 2017;29:1701627.
30. Zarek M, Mansour N, Shapira S, et al. 4D printing of shape memory-based personalized endoluminal medical devices. *Macromol Rapid Commun*. 2017;38: 1600628.
31. Ionita CN, Mokin M, Varble N, et al. Challenges and limitations of patient-specific vascular phantom fabrication using 3D Polyjet printing. *Proc SPIE-Int Soc Opt Eng*. 2014;9038:90380M.
32. Liu Y, Gao Q, Du S, et al. Fabrication of cerebral aneurysm simulator with a desktop 3D printer. *Sci Rep*. 2017;7:44301.
33. Li MH, Chen SW, Li YD, et al. Prevalence of unruptured cerebral aneurysms in Chinese adults aged 35 to 75 years: a cross-sectional study. *Ann Intern Med*. 2013; 159:514–521.
34. Frölich AM, Spallek J, Brehmer L, et al. 3D printing of intracranial aneurysms using fused deposition modeling offers highly accurate replications. *AJNR Am J Neuroradiol*. 2016;37:120–124.
35. Anderson JR, Thompson WL, Alkattan AK, et al. Three-dimensional printing of anatomically accurate, patient specific intracranial aneurysm models. *J Neurointerventional Surg*. 2015;8:517–520.
36. Kim PS, Choi CH, Han IH, et al. Obtaining informed consent using patient specific 3D printing cerebral aneurysm model. *J Korean Neurosurg Soc*. 2019;62:398–404.
37. Namba K, Higaki A, Kaneko N, et al. Microcatheter shaping for intracranial aneurysm coiling using the 3-dimensional printing rapid prototyping technology: preliminary result in the first 10 consecutive cases. *World Neurosurg*. 2015;84:178–186.
38. Xu C, Wang B, Han JY, et al. The application of 3D printing-assisted microcatheter shaping in the embolization of intracranial aneurysms. *J Intervent Radiol*. 2017;26: 1–5.
39. Xu Y, Tian W, Wei Z, et al. Microcatheter shaping using three-dimensional printed models for intracranial aneurysm coiling. *J Neurointerventional Surg*. 2019. https://doi.org/10.1136/neurintsurg-2019-015346.
40. Xie J, Li MH, Zhu YQ, et al. A new experimental model of intracranial internal carotid artery and its application in testing the navigability of the covered stents. *J Intervent Radiol*. 2009;18:136–140.
41. Martínez-Galdámez M, Escartín J, Pabón B, et al. Optical coherence tomography: translation from 3D-printed vascular models of the anterior cerebral circulation to the first human images of implanted surface modified flow diverters. *Intervent Neuroradiol*. 2019;25:150–156.
42. Kaneko N, Mashiko T, Namba K, et al. A patient-specific intracranial aneurysm model with endothelial lining: a novel in vitro approach to bridge the gap between biology and flow dynamics. *J Neurointerventional Surg*. 2018;10:306–309.
43. Shah A, Jankharia B, Goel A. Three-dimensional model printing for surgery on arteriovenous malformations. *Neurol India*. 2017;65:1350–1354.
44. Dong M, Chen G, Li J, et al. Three-dimensional brain arteriovenous malformation models for clinical use and resident training. *Medicine (Baltim)*. 2018;97, e9516.
45. Costa PF, Albers HJ, Linssen JEA, et al. Mimicking arterial thrombosis in a 3D-printed microfluidic in vitro vascular model based on computed tomography angiography data. *Lab Chip*. 2017;17:2785–2792.
46. Go AS, Mozaffarian D, Roger VL, et al. Heart disease and stroke statistics-2014 update: a report from the American Heart Association. *Circulation*. 2014;129: E28–E292.
47. Vukicevic M, Mosadegh B, Min JK, et al. Cardiac 3D printing and its future directions. *JACC Cardiovasc Imag*. 2017;10:171–184.
48. Dugas CM, Schussler JM. Advanced technology in interventional cardiology: a roadmap for the future of precision coronary interventions. *Trends Cardiovasc Med*. 2016;26:466–473.
49. Misra SK, Ostadhossein F, Babu R, et al. 3D-printed multidrug-eluting stent from graphene- nanoplatelet-doped biodegradable polymer composite. *Adv Healthcare Mater*. 2017;6:1700008.
50. Ge Q, Sakhaei AH, Lee H, et al. Multimaterial 4D printing with tailorable shape memory polymers. *Sci Rep*. 2016;6:31110.
51. Wang H, Liu J, Zheng X, et al. Three-dimensional virtual surgery models for percutaneous coronary intervention (PCI) optimization strategies. *Sci Rep*. 2015;5: 10945.

52. Velasco Forte MN, Byrne N, Valverde Perez I, et al. 3D printed models in patients with coronary artery fistulae: anatomical assessment and interventional planning. *EuroIntervention*. 2017;13:e1080–1083.
53. Farooqi KM, Saeed O, Zaidi A, et al. 3D printing to guide ventricular assist device placement in adults with congenital heart disease and heart failure. *JACC Heart Fail*. 2016;4:301–311.
54. Vukicevic M, Conover T, Jaeggli M, et al. Control of respiration-driven retrograde flow in the subdiaphragmatic venous return of the Fontan circulation. *Am Soc Artif Intern Organs J*. 2014;60:391–399.
55. Little SH, Vukicevic M, Avenatti E, et al. 3D printed modeling for patient-specific mitral valve intervention: repair with a clip and a plug. *J Am Coll Cardiol Intv*. 2016;9:973–975.
56. Vukicevic M, Puperi DS, Jane Grande-Allen K, et al. 3D printed modeling of the mitral valve for catheter-based structural interventions. *Ann Biomed Eng*. 2017;45:508–519.
57. Maragiannis D, Jackson MS, Igo SR, et al. Replicating patient-specific severe aortic valve stenosis with functional 3D modeling. *Circ Cardiovasc Imag*. 2015;8, e003626.
58. Qian Z, Wang K, Liu S, et al. Quantitative prediction of paravalvular leak in transcatheter aortic valve replacement based on tissue-mimicking 3D printing. *JACC Cardiovasc Imag*. 2017;10:719–731.
59. Armillotta A, Bonhoeffer P, Dubini G, et al. Use of rapid prototyping models in the planning of percutaneous pulmonary valved stent implantation. *Proc Inst Mech Eng H*. 2007;221:407–416.
60. Yuan D, Luo H, Yang H, et al. Precise treatment of aortic aneurysm by three-dimensional printing and simulation before endovascular intervention. *Sci Rep*. 2017;7:795.
61. Tam MD, Laycock SD, Brown JR, et al. 3D printing of an aortic aneurysm to facilitate decision making and device selection for endovascular aneurysm repair in complex neck anatomy. *J Endovasc Ther*. 2013;20:863–867.
62. Koleilat I, Jaeggli M, Ewing JA, et al. Interobserver variability in physician-modified endograft planning by comparison with a three-dimensional printed aortic model. *J Vasc Surg*. 2016;64:1789–1796.
63. Meess KM, Izzo RL, Dryjski ML, et al. 3D printed abdominal aortic aneurysm phantom for image guided surgical planning with a patient specific fenestrated endovascular graft system. *Proc SPIE-Int Soc Opt Eng*. 2017:10138.
64. Taher F, Falkensammer J, McCarte J, et al. The influence of prototype testing in three- dimensional aortic models on fenestrated endograft design. *J Vasc Surg*. 2017;65:1591–1597.
65. Rynio P, Kazimierczak A, Jedrzejczak T, et al. A 3-Dimensional printed aortic arch template to facilitate the creation of physician-modified stent-grafts. *J Endovasc Ther*. 2018;25:554–558.
66. Kärkkäinen JM, Sandri G, Tenorio ER, et al. Simulation of endovascular aortic repair using 3D printed abdominal aortic aneurysm model and fluid pump. *Cardiovasc Intervent Radiol*. 2019;42:1627–1634.
67. Ho D, Squelch A, Sun Z, et al. Modelling of aortic aneurysm and aortic dissection through 3D printing. *J Med Radiat Sci*. 2017;64:10–17.
68. Giannopoulos AA, Mitsouras D, Yoo SJ, et al. Applications of 3D printing in cardiovascular diseases. *Nat Rev Cardiol*. 2016;13:701–718.
69. Wu Z, Zhao J, Wu W, et al. Radial compressive property and the proof-of-concept study for realizing self-expansion of 3D printing polylactic acid vascular stents with negative Poisson's ratio structure. *Materials (Basel)*. 2018;11:1357.
70. Guerra AJ, Cano P, Rabionet M, et al. 3D-Printed PCL/PLA composite stents: towards a new solution to cardiovascular problems. *Materials (Basel)*. 2018;11:1679.
71. Oshiro Y, Ohkohchi N. Three-dimensional liver surgery simulation: computer-assisted surgical planning with three-dimensional simulation software and three-dimensional printing. *Tissue Eng A*. 2017;23:474–480.
72. von Rundstedt FC, Scovell JM, Agrawal S, et al. Utility of patient-specific silicone renal models for planning and rehearsal of complex tumor resections prior to robot-assisted laparoscopic partial nephrectomy. *BJU Int*. 2017;119:598–604.
73. Shibata E, Takao H, Amemiya S, et al. 3D-Printed visceral aneurysm models based on CT data for simulations of endovascular embolization: evaluation of size and shape accuracy. *AJR Am J Roentgenol*. 2017;209:243–247.
74. Takao H, Amemiya S, Shibata E, et al. 3D printing of preoperative simulation models of a splenic artery aneurysm: precision and accuracy. *Acad Radiol*. 2017;24:650–653.
75. Itagaki MW. Using 3D printed models for planning and guidance during endovascular intervention: a technical advance. *Diagn Interv Radiol*. 2015;21:338–341.
76. Nai QY, Ping J, Wei MX, et al. Application of 3D-printing technique in interventional treatment of Budd-Chiari syndrome: a preliminary study. *J Intervent Radiol*. 2017;26:732–735.
77. Witowski J, Darocha S, Kownacki Ł, et al. Augmented reality and three-dimensional printing in percutaneous interventions on pulmonary arteries. *Quant Imag Med Surg*. 2019;9:23–29.
78. Goudie C, Kinnin J, Bartellas M, et al. The use of 3D printed vasculature for simulation based medical education within interventional radiology. *Cureus*. 2019;11, e4381.
79. Zopf DA, Hollister SJ, Nelson ME, et al. Bioresorbable airway splint created with a three- dimensional printer. *N Engl J Med*. 2013;368:2043–2045.
80. Huang L, Wang L, He J, et al. Tracheal suspension by using 3-dimensional printed personalized scaffold in a patient with tracheomalacia. *J Thorac Dis*. 2016;8:3323–3328.
81. Guibert N, Didier A, Moreno B, et al. Treatment of post-transplant complex airway stenosis with a threedimensional, computer assisted customized airway stent. *Am J Respir Crit Care Med*. 2017;195:e31–e33.
82. Young BP, Machuzac MS, Gildea TR. Initial clinical experience using 3D printing and patient-specific airway stents: compassionate use of 3D printed patient-specific airway stents. *Am J Respir Crit Care Med*. 2017;195:A1711.
83. Guibert N, Moreno B, Hermant C. Usefulness of 3D printing to manage complex tracheal stenosis. *J Bronchol Interv Pulmonol*. 2017;24:e27–e29.
84. Jung SY, Lee SJ, Kim HY, et al. 3D printed polyurethane prosthesis for partial tracheal reconstruction: a pilot animal study. *Biofabrication*. 2016;8, 045015.
85. Lin M, Firoozi N, Tsai CT, et al. 3D-printed flexible polymer stents for potential applications in inoperable esophageal malignancies. *Acta Biomater*. 2019;83:119–129.
86. Boyer CJ, Boktor M, Samant H, et al. 3D printing for bio-synthetic biliary stents. *Bioengineering*. 2019;6:16.
87. Lee S, Ahn JY, Han M, et al. Efficacy of a three-dimensional-printed training simulator for endoscopic biopsy in the stomach. *Gut Liver*. 2018;12:149–157.
88. Pan TF, Lu J, Wang Y, et al. Clinical application of 3D printing template-assisted 125I radioactive seed interstitial brachytherapy in treating malignant tumors. *J Intervent Radiol*. 2018;27:740–744.
89. Liang YS, Wang J, Zhang HT, et al. The importance of template fixation in 3D printing individual template-guided 125I seed implantation for cephalocervical lymph node metastasis. *J Intervent Radiol*. 2018;27:745–749.
90. Li Q, Liang Y, Zhao Y, et al. Interpretation of adverse reactions and complications in Chinese expert consensus of Iodine-125 brachytherapy for pancreatic cancer. *J Canc Res Therapeut*. 2019;15:751–754.
91. Huang W, Lu J, Chen KM, et al. Preliminary application of 3D printing coplanar template in treating pancreatic cancer with 125I seed implantation. *J Intervent Radiol*. 2017;26:999–1003.
92. Guenette JP, Himes N, Giannopoulos AA, et al. Computer-based vertebral tumor cryoablation planning and procedure simulation involving two cases using MRI-Visible 3D printing and advanced visualization. *AJR Am J Roentgenol*. 2016;207:1128–1131.
93. Li J, Lin J, Yang Y, et al. 3-Dimensional printing guide template assisted percutaneous vertebroplasty: technical note. *J Clin Neurosci*. 2018;52:159–164.
94. van den Bos W, de Bruin DM, Jurhill RR, et al. The correlation between the electrode configuration and histopathology of irreversible electroporation ablations in prostate cancer patients. *World J Urol*. 2016;34:657–664.
95. Olweny EO, Kapur P, Tan YK, et al. Irreversible electroporation: evaluation of nonthermal and thermal ablative capabilities in the porcine kidney. *Urology*. 2013;81:679–684.
96. Wendler JJ, Klink F, Seifert S, et al. Irreversible electroporation of prostate cancer: patient- specific pretreatment simulation by electric field measurement in a 3D bioprinted textured prostate cancer model to achieve optimal electroporation parameters for image-guided focal ablation. *Cardiovasc Intervent Radiol*. 2016;39:1668–1671.